NASA/TM—2007-214847 AIAA–2007–1969

Probabilistic Simulation for Nanocomposite Characterization

Christos C. Chamis and Rula M. Coroneos
Glenn Research Center, Cleveland, Ohio

July 2007

NASA STI Program . . . in Profile

Since its founding, NASA has been dedicated to the advancement of aeronautics and space science. The NASA Scientific and Technical Information (STI) program plays a key part in helping NASA maintain this important role.

The NASA STI Program operates under the auspices of the Agency Chief Information Officer. It collects, organizes, provides for archiving, and disseminates NASA's STI. The NASA STI program provides access to the NASA Aeronautics and Space Database and its public interface, the NASA Technical Reports Server, thus providing one of the largest collections of aeronautical and space science STI in the world. Results are published in both non-NASA channels and by NASA in the NASA STI Report Series, which includes the following report types:

- TECHNICAL PUBLICATION. Reports of completed research or a major significant phase of research that present the results of NASA programs and include extensive data or theoretical analysis. Includes compilations of significant scientific and technical data and information deemed to be of continuing reference value. NASA counterpart of peer-reviewed formal professional papers but has less stringent limitations on manuscript length and extent of graphic presentations.

- TECHNICAL MEMORANDUM. Scientific and technical findings that are preliminary or of specialized interest, e.g., quick release reports, working papers, and bibliographies that contain minimal annotation. Does not contain extensive analysis.

- CONTRACTOR REPORT. Scientific and technical findings by NASA-sponsored contractors and grantees.

- CONFERENCE PUBLICATION. Collected papers from scientific and technical conferences, symposia, seminars, or other meetings sponsored or cosponsored by NASA.

- SPECIAL PUBLICATION. Scientific, technical, or historical information from NASA programs, projects, and missions, often concerned with subjects having substantial public interest.

- TECHNICAL TRANSLATION. English-language translations of foreign scientific and technical material pertinent to NASA's mission.

Specialized services also include creating custom thesauri, building customized databases, organizing and publishing research results.

For more information about the NASA STI program, see the following:

- Access the NASA STI program home page at *http://www.sti.nasa.gov*

- E-mail your question via the Internet to *help@sti.nasa.gov*

- Fax your question to the NASA STI Help Desk at 301–621–0134

- Telephone the NASA STI Help Desk at 301–621–0390

- Write to:
  NASA Center for AeroSpace Information (CASI)
  7115 Standard Drive
  Hanover, MD 21076–1320

NASA/TM—2007-214847 AIAA–2007–1969

Probabilistic Simulation for Nanocomposite Characterization

Christos C. Chamis and Rula M. Coroneos
Glenn Research Center, Cleveland, Ohio

Prepared for the
48th Structures, Structural Dynamics, and Materials (SDM) Conference
cosponsored by the AIAA, ASME, ASCE, AHS, and ASC
Honolulu, Hawaii, April 23–26, 2007

National Aeronautics and
Space Administration

Glenn Research Center
Cleveland, Ohio 44135

July 2007

This work was sponsored by the Fundamental Aeronautics Program
at the NASA Glenn Research Center.

Level of Review: This material has been technically reviewed by technical management.

Available from

NASA Center for Aerospace Information
7115 Standard Drive
Hanover, MD 21076–1320

National Technical Information Service
5285 Port Royal Road
Springfield, VA 22161

Available electronically at http://gltrs.grc.nasa.gov

Probabilistic Simulation for Nanocomposite Characterization

Christos C. Chamis and Rula M. Coroneos
National Aeronautics and Space Administration
Glenn Research Center
Cleveland, Ohio 44135

Abstract

A unique probabilistic theory is described to predict the properties of nanocomposites. The simulation is based on composite micromechanics with progressive substructuring down to a nanoscale slice of a nanofiber where all the governing equations are formulated. These equations have been programmed in a computer code. That computer code is used to simulate uniaxial strengths properties of a mononanofiber laminate. The results are presented graphically and discussed with respect to their practical significance. These results show smooth distributions.

Introduction

The research in the nanoscale technology has exploded over the recent past. An indication of this explosion is that the SAMPE (Society of Aerospace Material and Processing Engineers) Conference is devoting four sessions of about six papers each in the last 3 years. These papers cover practically all current research activities. The majority of the research is devoted to processing because of the difficulties involved in making a useful material (ref. 1). A few investigators have been fortunate to make some testing samples, which they subsequently tested to obtain limited data (ref. 2). A few other investigators researched the characterization of fatigue (ref. 3) and creep (ref. 4). A couple of papers explored the construction of nanocomposites for rocket ablative material (ref. 5) and for carbon nanotubes for adaptive structures (ref. 6). One paper ventured to describe a computer simulation of macroscopic properties of carbon nanotubes polymer composites (ref. 7). However, there are no results of what special macroscopic properties are included. Reference 7 shows one stress strain curve and citation of several references. One recent article (ref. 8) describes multiscale modeling and simulation of nanostructural materials from atomistic to micromechanics. This article does not include information on nanocomposites, but it mentions that mechanistic models will be needed in the end. It is becoming abundantly clear that no holistic approach has been used to investigate the mechanistic prediction of all nanocomposite uniaxial properties.

In this paper a unique mechanistic method is described to probabilistically simulate five uniaxial strengths and the transverse modulus of a mono nanofiber uniaxial composite. The mechanistic deterministic simulation of all uniaxial properties is described in reference 9.

Fundamentals

The fiber alignment with uniform dispersion is not met in nanocomposites. It is assumed herein that the fibers are aligned only for predicting “point” through-the-thickness properties. The fussiness can be simulated by estimating the angle of single fibers through the thickness. Therefore, it is assumed that an aligned unidirectional typical section of a nanocomposite is as illustrated schematically in figure 1 on the left 1(a). A nanoply is schematically shown in figure 1 on the right 1(b). It is interesting to note that in substructuring into slices, the monofiber nanoply is not constrained by the maximum fiber volume ratio, even though the monofiber was assumed to be in a square array with a limiting fiber volume ratio of about 0.78. The input includes the constituent material properties, tables I and II, the fabrication parameters, environmental, and the loading conditions.

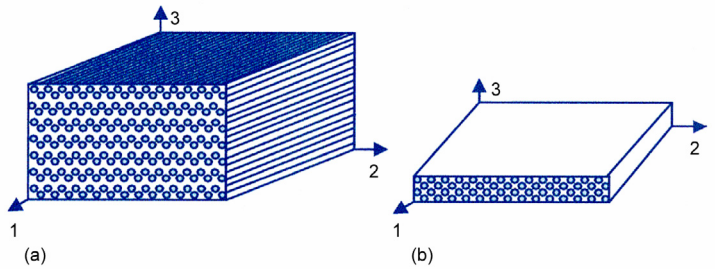

Figure 1.—Unidirectional nanocomposite typical section. (a) Nanocomposite. (b) Nanoply.

TABLE I.—T300 GRAPHITE NANOFIBER (PYROGRAF II) PROPERTIES
[Conversion Factors: 110 nm = 2.756×10^{-6} in.; psi = 6.89 Pa; lb/in.^{3} = 1146 kg/cm^3; in./in./°f = (2/5); cm/cm/°c; btu = 1055 joules.]

Description	Symbol	Value	Units
Number of fibers per end	Nf	1.0	number
Filament equivalent diameter	df	2.756×10^{-6}	in.
Weight density	Rhof	0.064	lb/in.**3
Normal moduli (11)	Ef11	1.0×10^{9}	psi
Normal moduli (22)	Ef22	7.0×10^{7}	psi
Poisson's ratio (12)	Nuf12	0.2	Nondimensional
Poisson's ratio (23)	Nuf23	0.25	Nondimensional
Shear moduli (12)	Gf12	5.0×10^{7}	psi
Shear moduli (23)	Gf23	3.5×10^{7}	psi
Thermal expansion coefficient (11)	A1faf11	-5.5×10^{-7}	in./in./°F
Thermal expansion coefficient (22)	Alfaf22	5.6×10^{-6}	in./in./°F
Heat conductivity (11)	Kf11	444.0	Btu/hr/ft^2/°F/in.
Heat conductivity (22)	Kf22	4.0	Btu/hr/ft^2/°F/in.
Heat capacity	Cf	0.22	Btu/lb/°F
Dielectric strength (11)	KeF11	0.0	V/in.
Dielectric strength (22)	Kef22	0.0	V/in.
Dielectric constant (11)	Gamma11	0.0	in./V
Dielectric constant (22)	Gamma22	0.0	in./V
Capacitance	Cef	0.0	V
Resistivity	Ref	0.0	Ω-in.
Tensile strength	SfT	8.0×10^{5}	psi
Compressive strength	SiC	6.0×10^{5}	psi
Shear strength	SfS	4.0×10^{5}	psi
Normal damping capacity (11)	psi11f	0.38	%Energy
Normal damping capacity (22)	psi22f	6.3	%Energy
Shear damping capacity (12)	psi12f	3.34	%Energy
Shear damping capacity (23)	psi23f	6.3	%Energy
Melting temperature	TMf	6000.0	°F

TABLE II.—INTERMEDIATE MODULUS HIGH-STRENGTH MATRIX (EPOXY)
[Conversion Factors: 110 nm = 2.756×10^{-6} in.; psi = 6.89 Pa; lb/in^3 = 1146 kg/cm^3; in./in./°F = (2/5); cm/cm/°C; btu = 1055 joules]

Description	Symbol	Value	Units
Weight density	Rhom	0.044	lb/in.**3
Normal modulus	Em	500000.0	psi
Poisson's ratio	Num	0.35	Nondimensional
Thermal expansion coefficient	Alfa m	3.6×10^{-5}	in./in./°F
Heat conductivity	Km	0.008681	Btu/hr/ft^2/°F/in.
Heat capacity	Cm	0.25	Btu/lb/°F
Dielectric strength	Kem	0.0	V/in.
Dielectric constant	Gammam	0.0	in./V
Capacitance	Cem	0.0	V
Resistivity	Rem	0.0	Ω-in.
Moisture expansion coefficient	Betam	0.0033	in./in./%moisture
Diffusivity	Dm	2.16×10^{-7}	in.**2/hr
Saturation	Mm	0.0	%moisture
Tensile strength	SmT	15000.0	psi
Compressive strength	SmC	35000.0	psi
Shear strength	SmS	13000.0	psi
Allowable tensile strain	eps mT	0.02	in./in.
Allowable compression strain	eps mC	0.05	in./in.
Allowable shear strain	eps mS	0.035	in./in.
Allowable torsional strain	eps mTOR	0.035	in./in.
Normal damping capacity	psiNM	6.6	%energy
Shear damping capacity	psiSm	6.9	%energy
Void heat conductivity	Kv	0.0012	Btu/hr/in./°F
Glass transition temperature	Tgdr	420.0	°F
Melting temperature	TMm	0.0	°F

The properties prediction is expedited by the following geometric diagrams: An exploded view of nanoscale isolation of a typical part is shown in figure 2 with nanoscale dimensions. A single nanofiber schematic with substructuring is shown in figure 3(a), and a typical subslice is shown in figure 3(b).

A nanosubply with its corresponding stresses is shown in figure 4. The nanomechanics predictive equations are derived by using figure 4. The equations used are all programmed in ICAN/JAVA (ref. 10). A limited set of equations used for this paper are summarized in the appendix.

Prior to describing the results obtained, it is instructive to describe the interphase and how it is modeled. The schematics in figure 5 show a vertical section, upper figure part, with unit thickness of the nanocomposite and a single fiber in it. As can be seen in the slice, lower figure, the fiber interphase is represented by a series of progressively larger volume voids starting with the smallest near the matrix interface and ending with the largest in the fiber interface. It can be visualized that the stress in the matrix will be magnified because of the voids. This magnification is shown in figure 6 for a specific nanocomposite with 0.05 fiber volume ratio and with void volume ratio varying from 0.05 to 0.4. The interesting point to note in the lower part of figure 5 is that the matrix is continuous even though it is filled with progressively larger voids; otherwise the stresses will not be continuous in the matrix.

It is instructive to elaborate a bit further with the geometry of figure 5, lower part. In order to fill up a conventional ply of 0.005 in. thick and a width of 1 in., it will require about 1×10^6 fibers, a very large number indeed. The magnification factor of the voids effect in the interphase is show in figure 6. As can be seen in figure 6, the magnification factor increases from a value of about 1.1 to a maximum of about 2. Therefore, the maximum void effect will be nearest to the fiber interface.

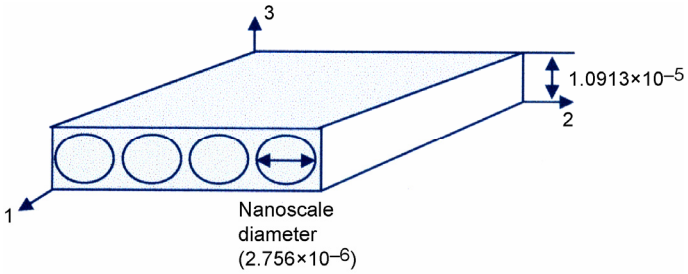

Figure 2.—Nanoscale isolation of a typical part (units are in in.).

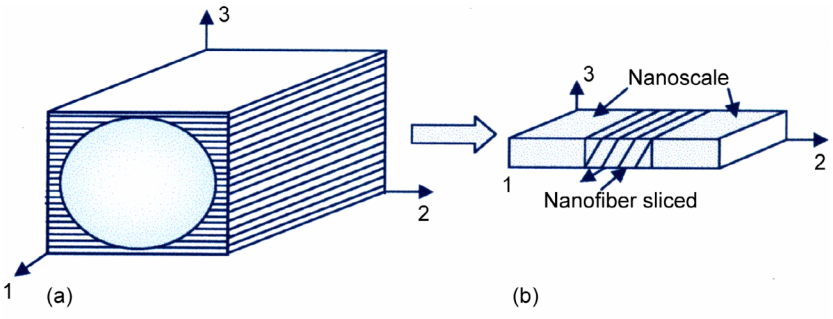

Figure 3.—Nanofiber substructuring. (a) Several slices through the thickness. (b) Nanofiber sliced.

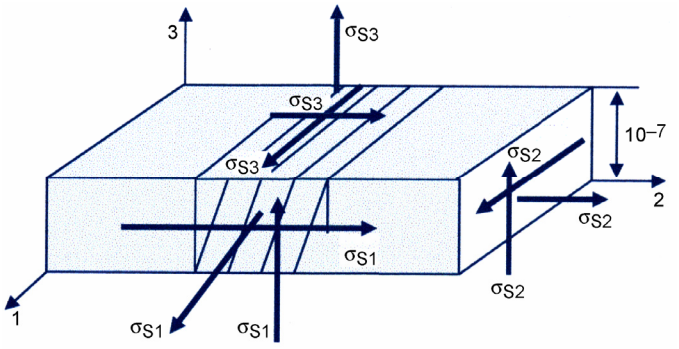

Figure 4.—Nanostresses on a nanosubply (units are in in.).

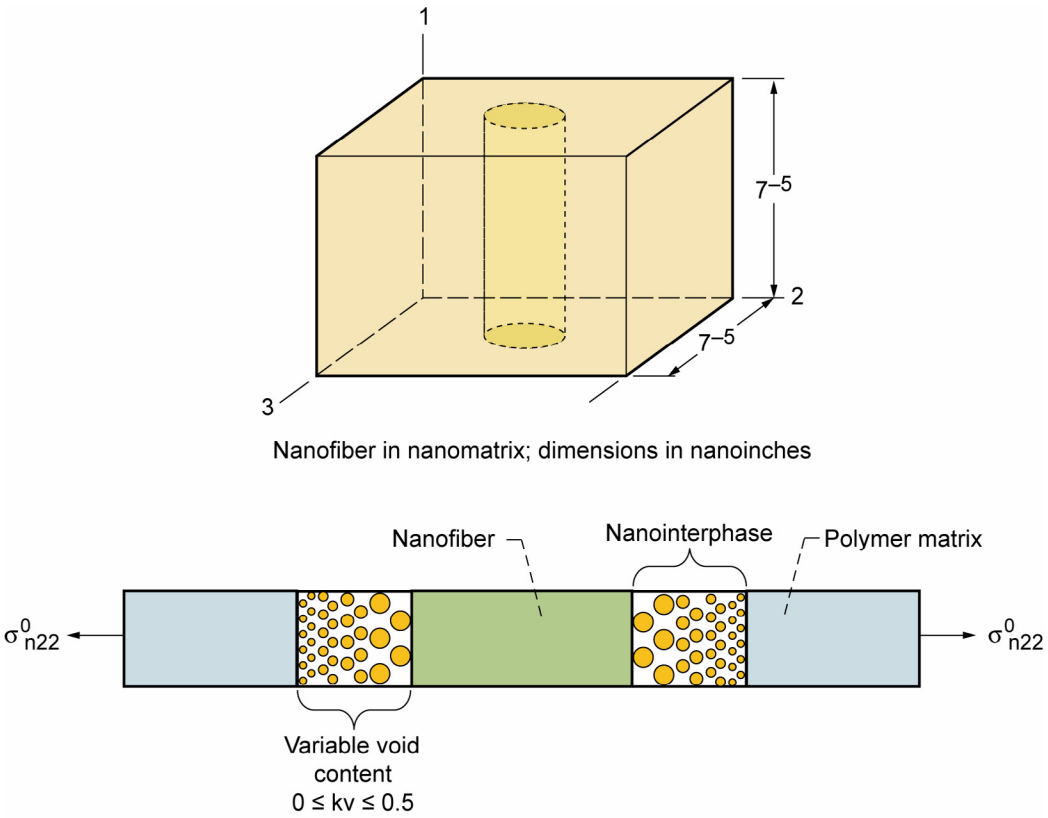

Figure 5.—Vertical section a composite nanocell through nanofiber center.

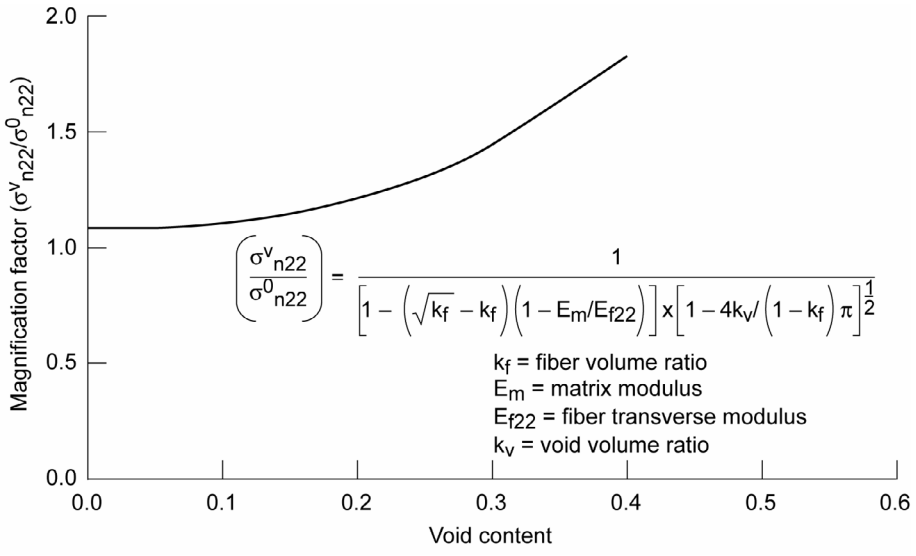

Figure 6.—Nanocomposite magnification factor.

Results and Discussion

In this section the probabilistic results are presented and discussed starting with the large voids in the interphase. The probabilistic void magnification factor is shown graphically in figure 7. It can be seen in figure 7 that the larger the void content the greater the deviation. The left most figure is closest to the matrix interphase interface while the right most curve is closest to the interphase interface. The respective scatter is about 0.1 for the curve closest to the matrix to about 1 for the curve closest to the fiber. The corresponding sensitivities are shown in figure 8. It can be seen in this figure that the void sensitivities on the magnification factor is large. The probabilistic void effects on the uniaxial strengths are plotted in figure 9. Figure 9(a) shows the spread in the longitudinal tensile strength; figure 9(b), in the longitudinal compressive strength; figure 9(c), in the transverse tensile strength and figure 9(d) in the transverse compressive strength. It can be seen in figure 9 that the distribution for the two longitudinal strengths is relatively large. It is from 150 to 650 ksi, for tensile strength and with a distribution of about 500 ksi, and for the compressive strength is from 140 to 500 ksi or a distribution of about 360 ksi. The corresponding probabilistic sensitivities are plotted in figure 10 for tensile and figure 11 for compressive. It can be seen in these two figures that there is no difference in the sensitivities for the three probabilities.

The probabilistic intralaminar shear strength is plotted in figure 12. The distribution in this strength is from about 6,000 to ~16,000 psi or ~10 ksi spread. It is a relatively wide distribution from lowest probability to the highest. The corresponding probability sensitivities are plotted in figure 13 for uniaxial nano transverse tensile strength. Note that these probabilistics are for 0.0001, 0.50, and 0.9999. They are about the same and may be easily interchangeable as well as for three fiber volume ratios.

The corresponding sensitivities for the nano uniaxial compressive strength are plotted in figure 14 for three probabilities, as was the case for the transverse tensile; these sensitivities are also the same and can easily be interchangeable. The corresponding sensitivities for the nano intralaminar sheer strength are plotted in figure 15. As was the case for the previous sensitivities, these sensitivities are also about the same and can easily be interchanged. The probabilistic transverse modulus is plotted in figure 16. The scatter is from 225 to ~650 ksi or a distribution of ~425 ksi.

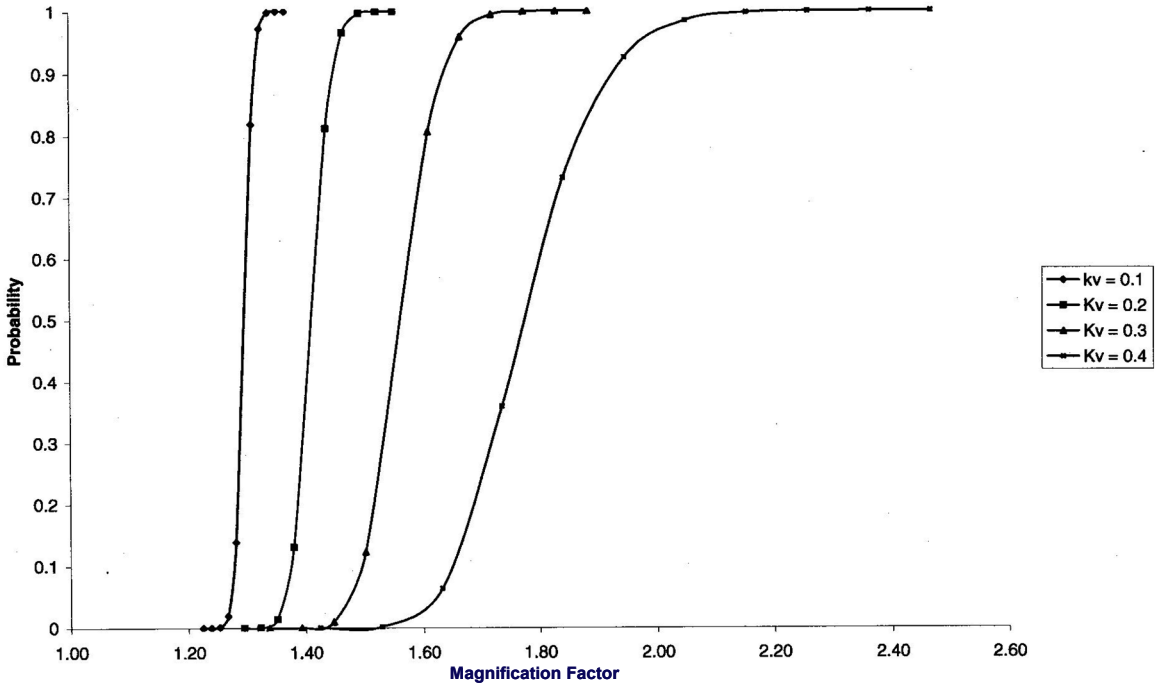

Figure 7.—Probabilistic magnification factor of voids in the interphase.

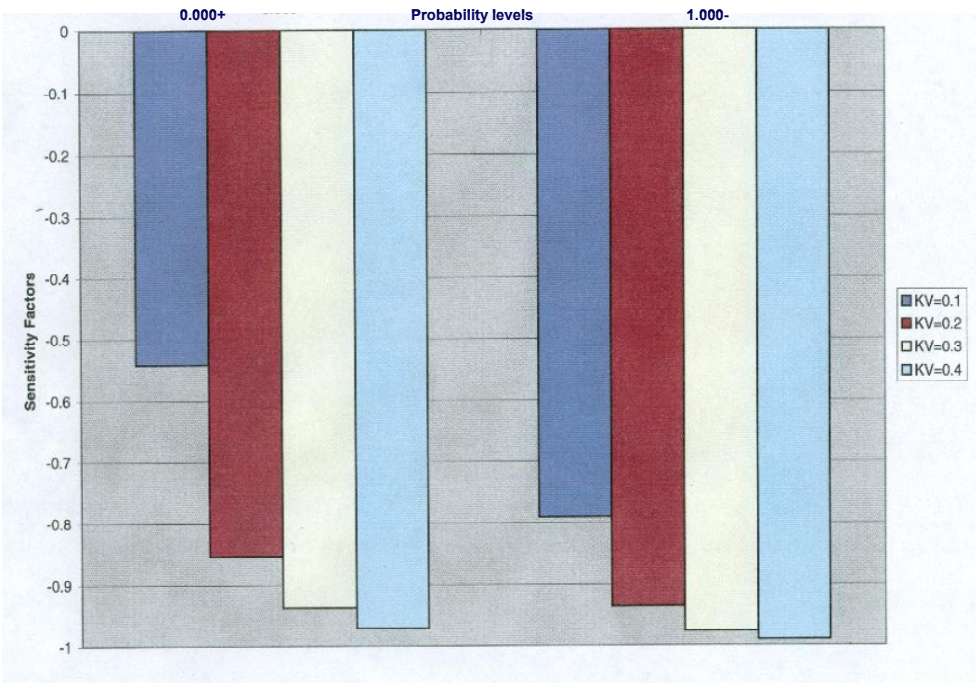

Figure 8.—Voids sensitivities on the interphase magnification factor.

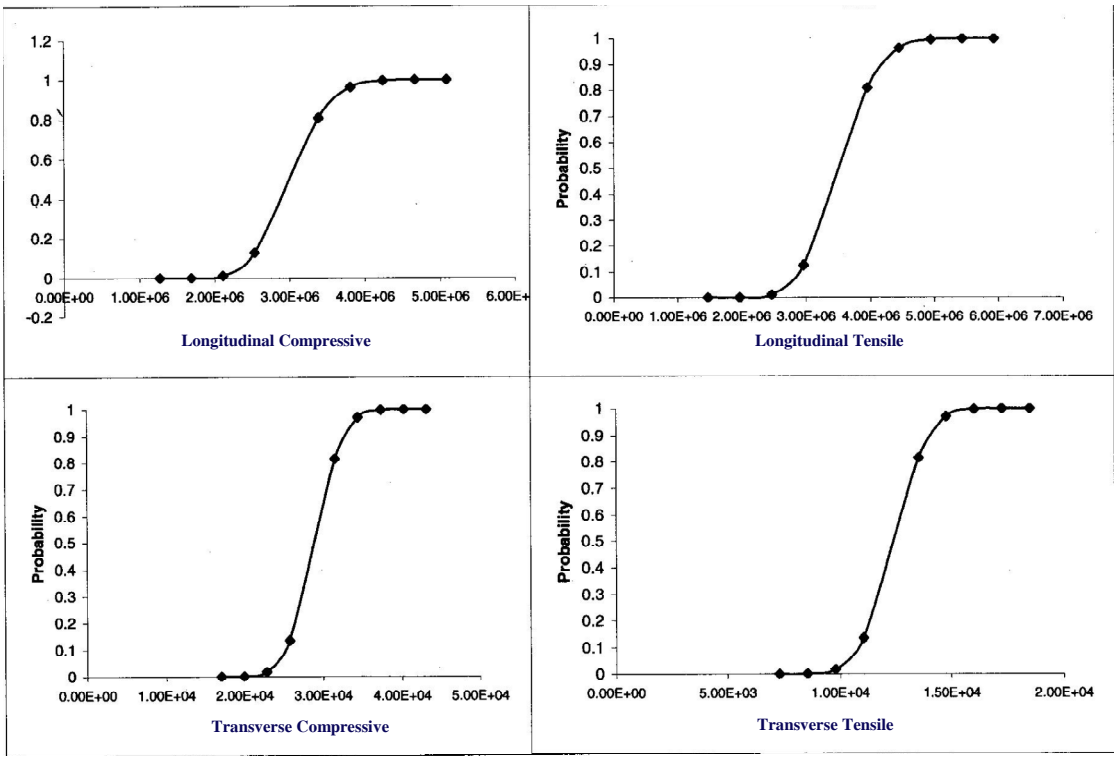

Figure 9.—Probabilistically plotted nano uniaxial strengths.

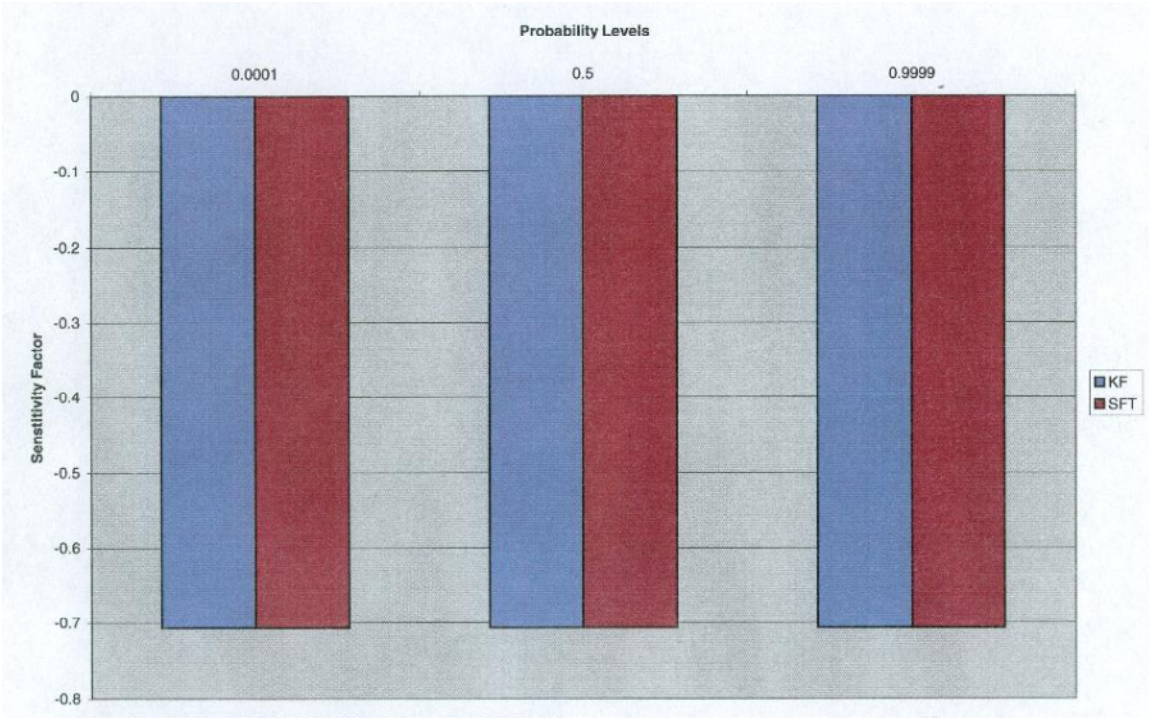

Figure 10.—Probabilistic sensitivities for nano longitudinal uniaxial strength.

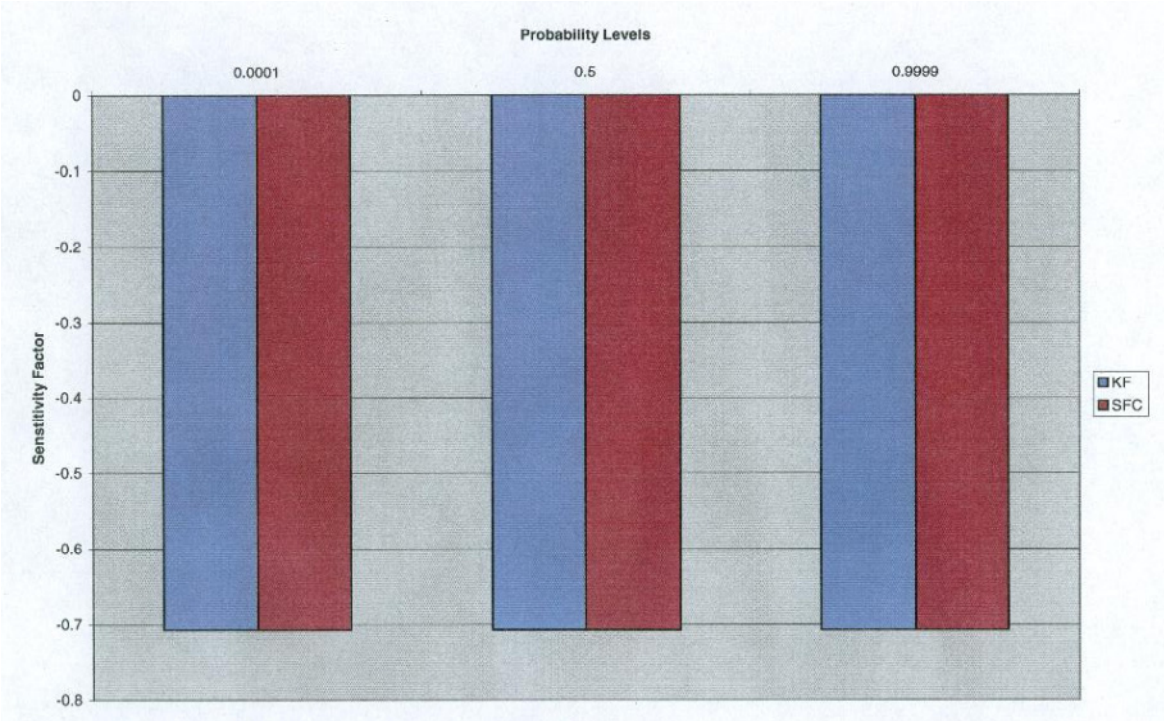

Figure 11.—Probabilistic sensitivities for the nano compressive uniaxial strength.

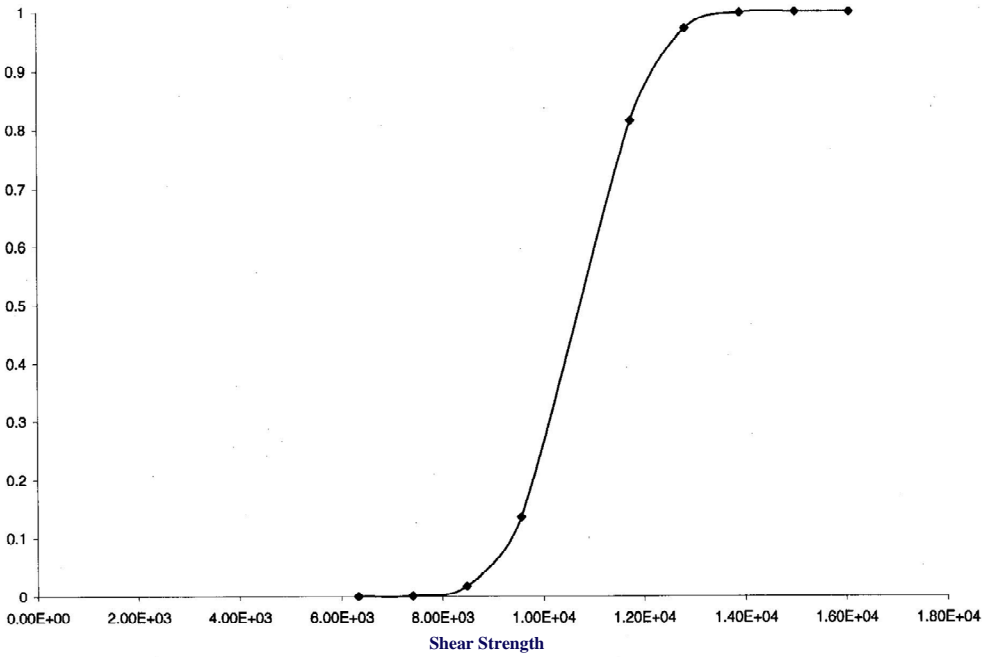

Figure 12.—Probabilistically plotted intralaminar uniaxial shear strength.

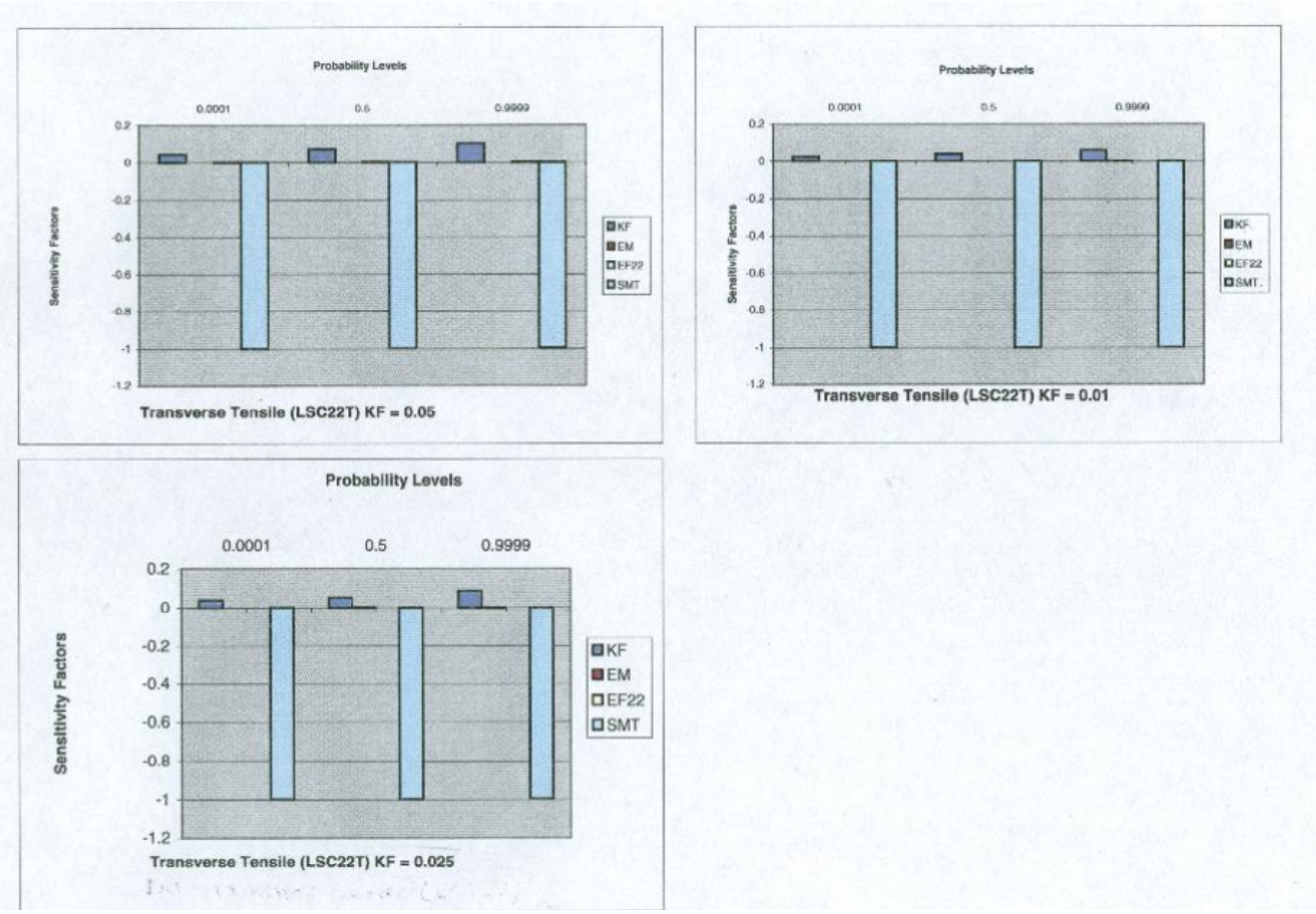

Figure 13.—Probabilistic sensitivities for nano uniaxial transverse tensile strength for three different probabilities.

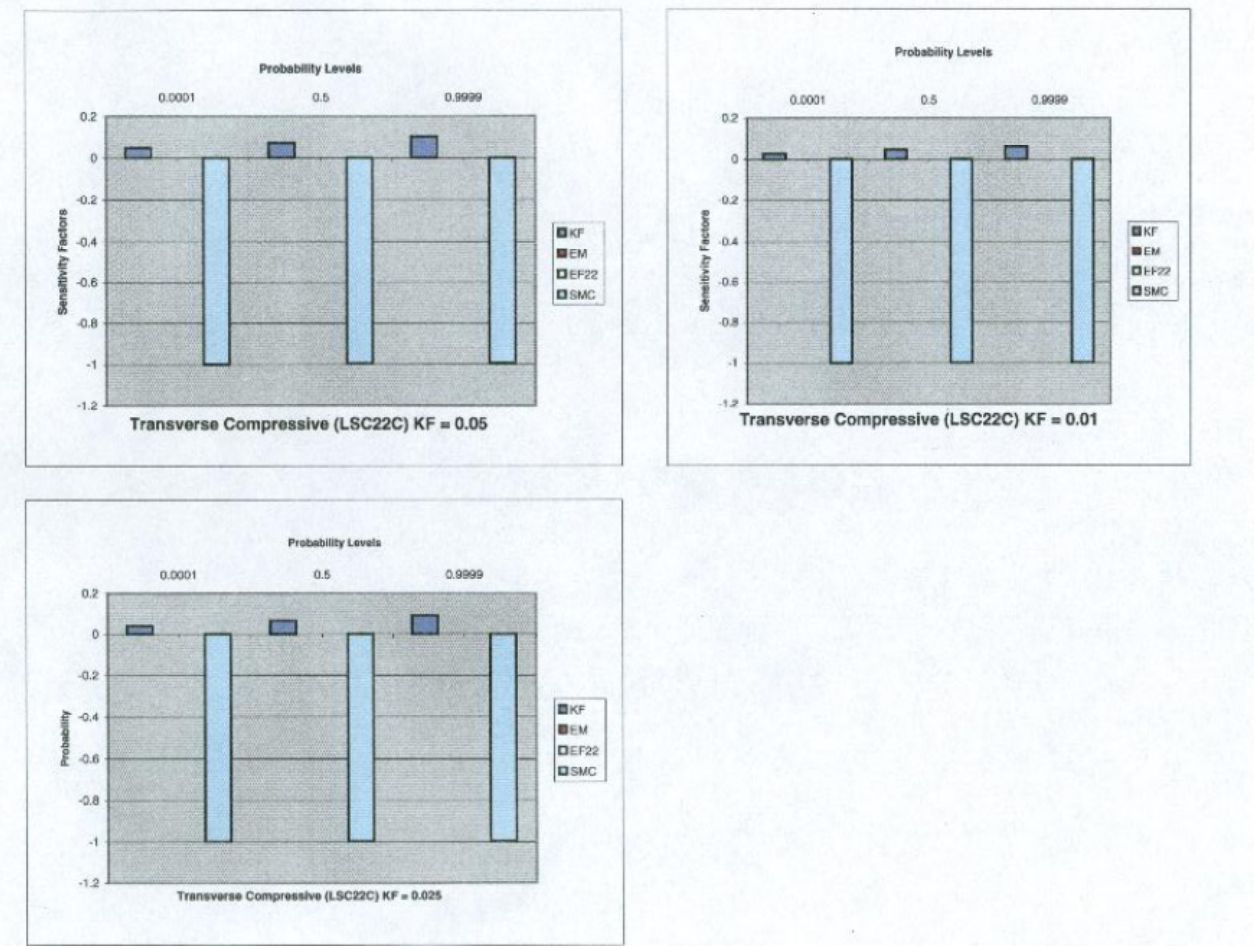

Figure 14.—Probabilistic sensitivities for nano uniaxial transverse compressive strength for three different probabilities.

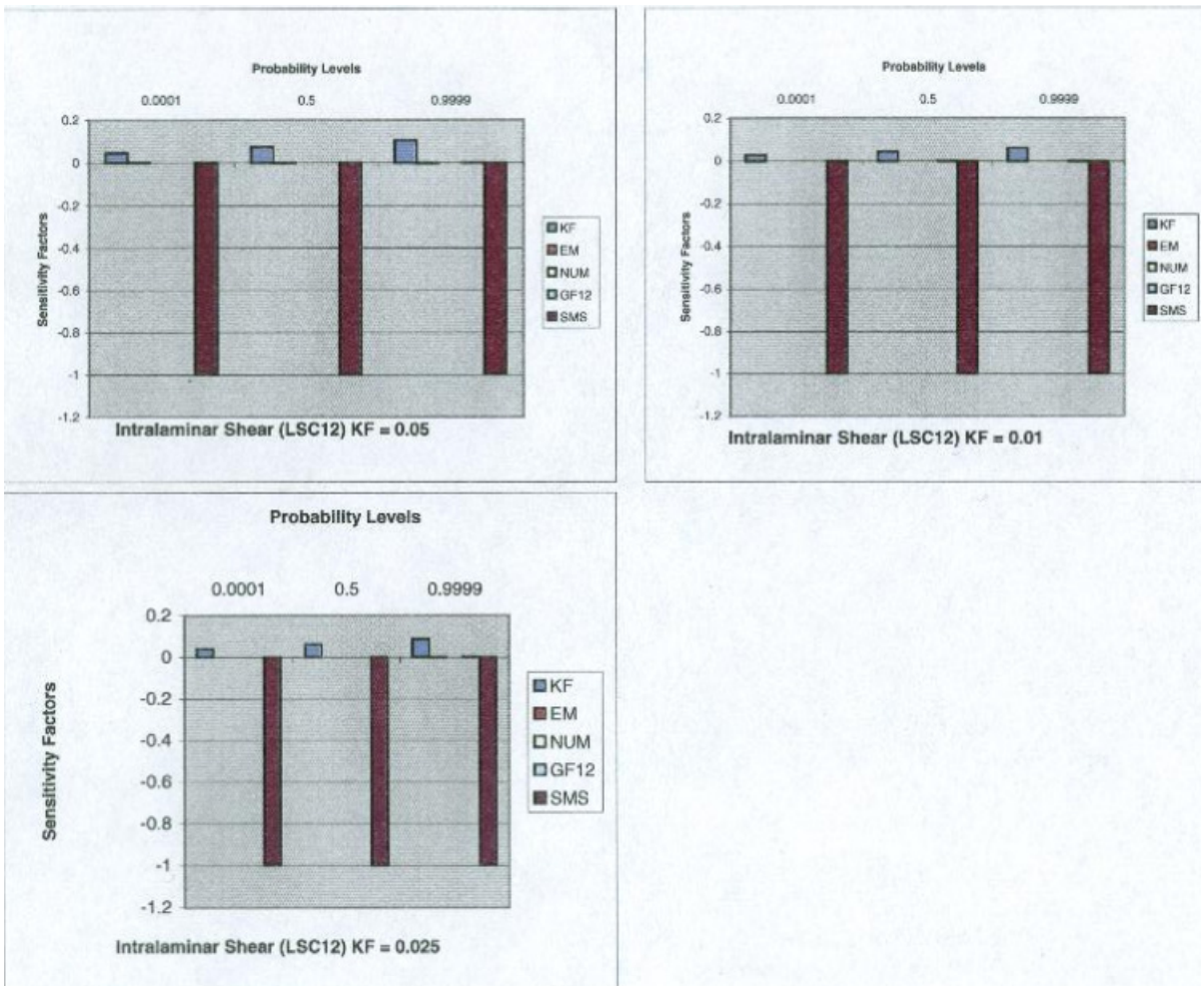

Figure 15.—Probabilistic sensitivities for nano intralaminar shear strength for three different probabilities.

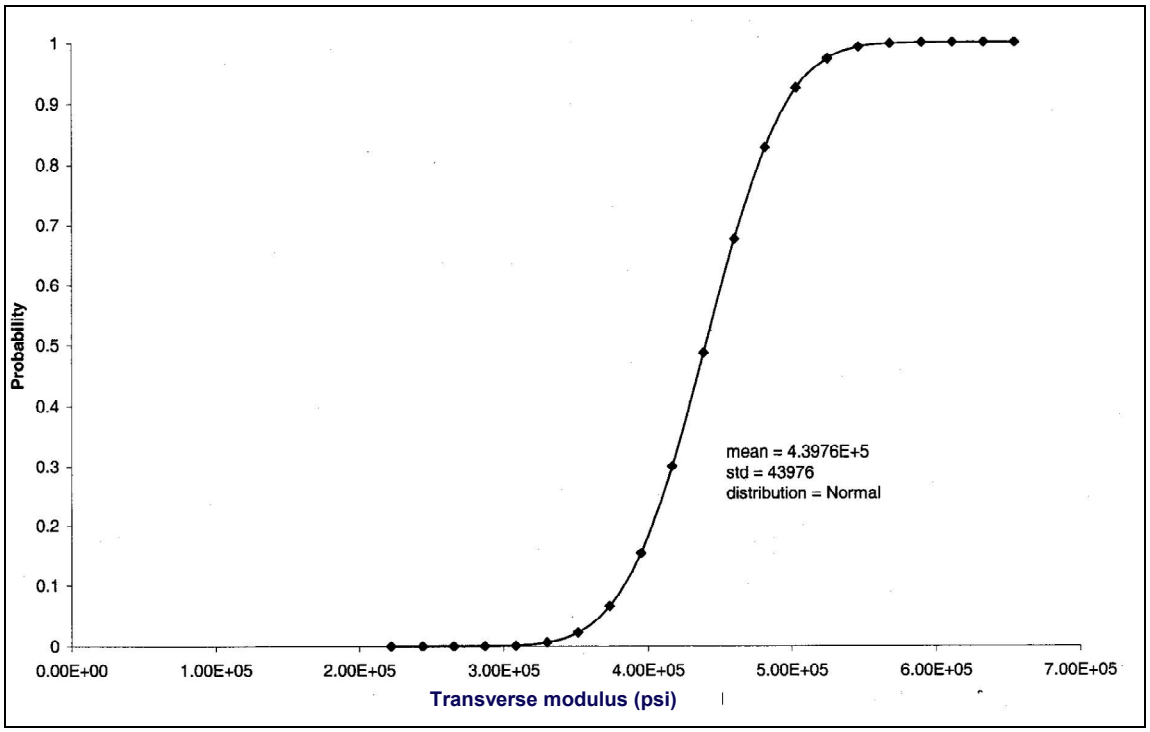

Figure 16.—Probabilistically plotted nano transverse modulus.

Concluding Remarks

The salient remarks from an investigation to characterize an aligned monofiber nanolaminate are as follows:

1. The characterization for the nanolaminate (composite) was based on a series of progressive substructuring down a sliced single-diameter fiber.
2. The theoretical development and all the equations are included in a computer code called ICAN/JAVA.
3. The characterization includes two fabrication parameters, 5-nano uniaxial strengths and the transverse modulus.
4. The nanolaminate investigated consists of single nanofiber laminate with 0.05 fiber volume ratio.
5. The effects of the interphase are especially important and are represented by progressively large amounts of voids from the matrix interface to the fiber interphase.
6. The probabilistic evaluation characterizes the effects of uncertainties in all participating variables.
7. The voids uncertainties indicate as the void volume ratio increases the distribution increases as well.
8. The voids contribute significantly to matrix dominated strengths.

Appendix—Equations Used in the Nanomechanic Characterization

Partial volumes $k_f + k_m + k_v = 1$

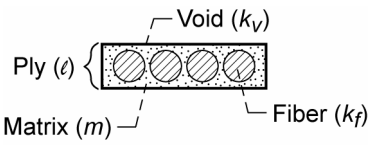

Ply density $\rho_\ell = k_f \rho_f + k_m \rho_m$

Resin volume ratio $k_m = (1 - k_v) / \left[1 + (\rho_m / \rho_f)(1/\lambda_m - 1)\right]$

Fiber volume ratio $k_f = (1 - k_v) / \left[1 + (\rho_f / \rho_m)(1/\lambda_f - 1)\right]$

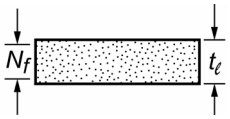

Weight ratios $\lambda_f + \lambda_m = 1$

Ply thickness (S.A.) $t_\ell = 1/2\, N_f\, d_f \sqrt{\pi / k_f}$

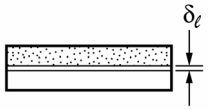

Interply thickness $\delta_\ell = 1/2 \left[\sqrt{\pi / k_f} - 2\right] d_f$

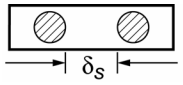

Interfiber spacing (S.A.) $\delta_s = \delta_\ell$

Contiguous fibers (S.A.) $k_f = \pi/4 \sim 0.785$

(a) Micromechanics and geometric relationships.

Longitudinal modulus $E_{\ell 11} = k_f\, E_{f11} + k_m\, E_m$

Transverse modulus $E_{\ell 22} = \dfrac{E_m}{1 - \sqrt{k_f}\left(1 - E_m / E_{f22}\right)} = E_{\ell 33}$

Shear modulus $G_{\ell 12} = \dfrac{G_m}{1 - \sqrt{k_f\left(1 - G_m / G_{f12}\right)}} = G_{\ell 13}$

Shear modulus $G_{\ell 23} = \dfrac{G_m}{1 - \sqrt{k_f\left(1 - G_m / G_{f23}\right)}}$

Poisson's ratio $\nu_{\ell 12} = k_f\ \nu_{f12} + k_m\ \nu_m = \nu_{\ell 13}$

Poisson's ratio $\nu_{\ell 23} = \dfrac{E_{\ell 22}}{2G_{\ell 23}} - 1$

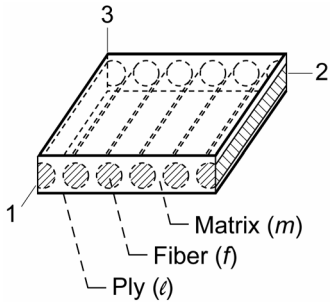

(b) Composite mechanical properties.

Longitudinal tension $S_{\ell 11T} \approx k_f S_{fT}$

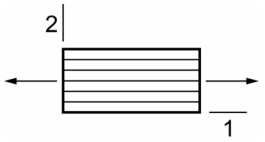

Longitudinal compression

Fiber compression $S_{\ell 11C} \approx k_f S_{fC}$

Delamination/shear $S_{\ell 11C} \approx 10 S_{\ell 12S} + 2.5\ S_{mT}$

Microbuckling $S_{\ell 11C} \approx \dfrac{G_m}{1 - k_f\left(1 - \dfrac{G_m}{G_{f12}}\right)}$

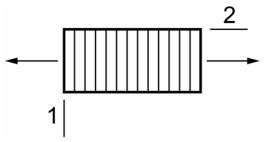

Transverse tension $S_{\ell 22T} \approx \left[1 - \left(\sqrt{k_f} - k_f\right)\left(1 - E_m / E_{f22}\right)\right] S_{mT}$

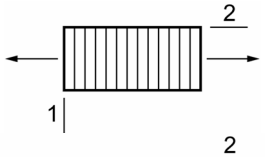

Transverse compression $S_{\ell 22C} \approx \left[1 - \left(\sqrt{k_f} - k_f\right)\left(1 - E_m / E_{f22}\right)\right] S_{mC}$

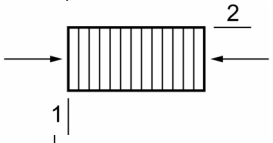

Intralaminar shear $S_{\ell 12S} \approx \left[1 - \left(\sqrt{k_f} - k_f\right)\left(1 - G_m / G_{f12}\right)\right] S_{mS}$

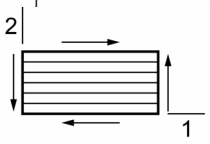

For voids $S_m \approx \left\{1 - \left[4k_v / \left(1 - k_f\right)\pi\right]^{1/2}\right\} S_m$

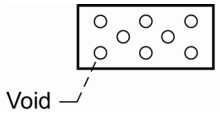

(c) Composite uniaxial strengths, in-plane.

References

1. Jose, M., Tyner, J., Nyairo, E., and Dean, D., "Synthesis and Processing of Aligned Carbon Nanotube Based Fibers," presented at the *49th International SAMPE Symposium and Exhibition*, (CD). May 16–20, 2004.
2. Ayalasomayajuala, G., Garg, A., Kapila, S., Chandrashekhara, K., and Flanigan, V., "Fabrication and Evaluation of Rice Hull Derived Nano Silica Composites," presented at the *49th International SAMPE Symposium and Exhibition* (CD). May 16–20, 2004.
3. Karaki, T., Killgore, J.P., and Seferis, J.C., "Characterization of Fatigue Behavior of Polynanomeric Matrix Composites," presented at the *49th International SAMPE Symposium and Exhibition* (CD). May 16–20, 2004.
4. Ranade, A., D'Souza, N.A., Nayak, K., Gnade, B., and Fairbrother, D., 2003. Correlation Between Creep-Recovery, Crystallization and Dispersion of Linear Low Density Polyethylene Nanocomposite Films, *48th International Symposium and Exhibition*, vol. 48, book 1 of 2, pp. 2164–2176.
5. Koo, J.H., Stretz, H., Weispfenning, J., Luo, Z.P., and Wootan, W., "Nanocomposite Rocket Ablative Materials: Subscale Ablation Test," presented at the *49th International SAMPE Symposium and Exhibition*, (CD). May 16–20, 2004.
6. Muhle, S., Monner, H.P., and Wiersch, P., 2003. Carbon-Nanotubes for Adaptive Structures, *48th International SAMPE Symposium and Exhibition,* vol. 48, book 1 of 2, pp. 1181–1190.
7. Srivastava, D. and Wei, C., 2003. Computer Simulations of Macroscopic Properties of Carbon-Nanotube Polymer Composites, *48th International SAMPE Symposium and Exhibition*, vol. 48, book 1 of 2, pp. 2153–2163.
8. Gates, T.S., et al., "Computational Materials: Multi-scale Modeling and Simulation of Nanostructural Materials." *Composites Science and Technology*, 65 (2005), pp. 2416–2434.
9. Chamis, C.C., Composite Nanomechanics Properties Prediction, NASA/TM—2007-214673, February 2007.
10. Handler, L.M. and Chamis, C.C., ICAN/JAVA Computer Code.

REPORT DOCUMENTATION PAGE	Form Approved OMB No. 0704-0188

1. REPORT DATE *(DD-MM-YYYY)*	2. REPORT TYPE	3. DATES COVERED *(From - To)*
17-07-2007	Technical Memorandum	

4. TITLE AND SUBTITLE
Probabilistic Simulation for Nanocomposite Characterization

5a. CONTRACT NUMBER

5b. GRANT NUMBER

5c. PROGRAM ELEMENT NUMBER

6. AUTHOR(S)
Chamis, Christos, C.; Coroneos, Rula, M.

5d. PROJECT NUMBER

5e. TASK NUMBER

5f. WORK UNIT NUMBER
WBS 561581.02.08.03.15.03

7. PERFORMING ORGANIZATION NAME(S) AND ADDRESS(ES)
National Aeronautics and Space Administration
John H. Glenn Research Center at Lewis Field
Cleveland, Ohio 44135-3191

8. PERFORMING ORGANIZATION REPORT NUMBER
E-16063

9. SPONSORING/MONITORING AGENCY NAME(S) AND ADDRESS(ES)
National Aeronautics and Space Administration
Washington, DC 20546-0001

10. SPONSORING/MONITORS ACRONYM(S)
NASA

11. SPONSORING/MONITORING REPORT NUMBER
NASA/TM-2007-214847; AIAA-2007-1969

12. DISTRIBUTION/AVAILABILITY STATEMENT
Unclassified-Unlimited
Subject Category: 24
Available electronically at http://gltrs.grc.nasa.gov
This publication is available from the NASA Center for AeroSpace Information, 301-621-0390

13. SUPPLEMENTARY NOTES

14. ABSTRACT
A unique probabilistic theory is described to predict the properties of nanocomposites. The simulation is based on composite micromechanics with progressive substructuring down to a nanoscale slice of a nanofiber where all the governing equations are formulated. These equations have been programmed in a computer code. That computer code is used to simulate uniaxial strengths properties of a mononanofiber laminate. The results are presented graphically and discussed with respect to their practical significance. These results show smooth distributions.

15. SUBJECT TERMS
Nanofiber; Nanolaminate; Nano uniaxial strength; Interphase effects; Probabilistic simulation; Probabilistic sensitivities

16. SECURITY CLASSIFICATION OF:			17. LIMITATION OF ABSTRACT	18. NUMBER OF PAGES	19a. NAME OF RESPONSIBLE PERSON
a. REPORT	b. ABSTRACT	c. THIS PAGE			Christos C. Chamis
U	U	U		21	19b. TELEPHONE NUMBER *(include area code)* 216-433-3252